Supplement of Atmos. Chem. Phys., 23, 3731–3748, 2023
https://doi.org/10.5194/acp-23-3731-2023-supplement

Atmospheric Chemistry and Physics
Open Access
EGU

Supplement of

Improving ozone simulations in Asia via multisource data assimilation: results from an observing system simulation experiment with GEMS geostationary satellite observations

Lei Shu et al.

Correspondence to: Lei Zhu (zhul3@sustech.edu.cn)

Table S1. WRF-Chem and GEOS-Chem model configurations.

Configurations	(1) WRF-Chem v4.1	(2) GEOS-Chem v12.9.3
Global simulation	—	2° × 2.5° with 72 vertical layers up to 0.1 hPa, spin-up time of 1 year
Asian simulation	50 km × 50 km (centered at 35°N, 103°E) with 34 vertical layers up to 50 hPa, spin-up time of 72 h	0.5° × 0.625° (11°S–55°N, 60°–150°E) with 47 vertical layers up to 0.1 hPa, boundary conditions updated every 3 h from the global simulation, spin-up time of 6 months
Meteorological conditions	National Centers for Environmental Prediction (NCEP) Final (FNL) operational global analysis (https://rda.ucar.edu/datasets/ds083-3/, last access: 1 March 2023), 0.25° × 0.25°	Modern-Era Retrospective Analysis for Research and Applications, Version 2 (MERRA-2) meteorological fields (Gelaro *et al.*, 2017)
Chemical initial and boundary conditions	Whole Atmosphere Community Climate Model (WACCM) 6 h outputs (Gettelman *et al.*, 2019)	—
Anthropogenic emission	Multi-resolution Emissions Inventory for China (MEIC) (Zheng *et al.*, 2018), 0.25° × 0.25°; Emissions Database for Global Atmospheric Research-Hemispheric Transport of Air Pollution (EDGAR-HTAP) (Janssens-Maenhout *et al.*, 2015) outside China, 1° × 1°	Community Emissions Data System (CEDS) (Hoesly *et al.*, 2018), substituted by MIX inventory (Li *et al.*, 2017) over Asia
Biogenic emission	Model of Emissions of Gases and Aerosols from Nature (MEGAN) (Guenther *et al.*, 2012)	MEGAN
Fire emission	Fire INventory from NCAR (FINN) version 1.5 (Wiedinmyer *et al.*, 2011)	the fourth-generation Global Fire Emissions Database (GFED4) (Giglio *et al.*, 2013)
Chemical mechanism	CBMZ chemical mechanism (Zaveri and Peters, 1999) for gas-phase chemistry and MOSAIC aerosol scheme configured with 4 sectional aerosol bins (Zaveri *et al.*, 2008)	HO_x-NO_x-VOC-ozone-aerosol-halogen tropospheric chemistry mechanism (Bey *et al.*, 2001; Park *et al.*, 2004; Mao *et al.*, 2013)

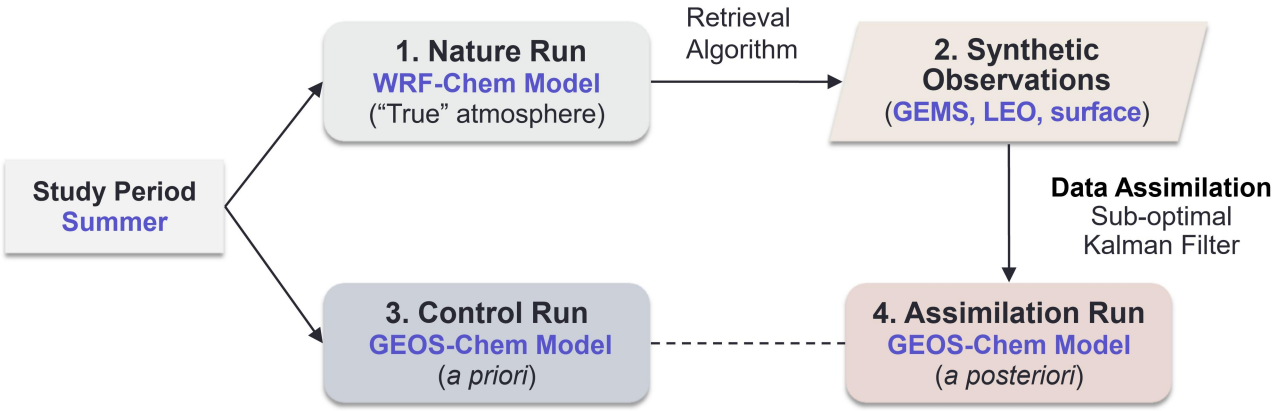

Figure S1. The framework of the Observing System Simulation Experiment (OSSE). Modified from Shu *et al.* (2022).

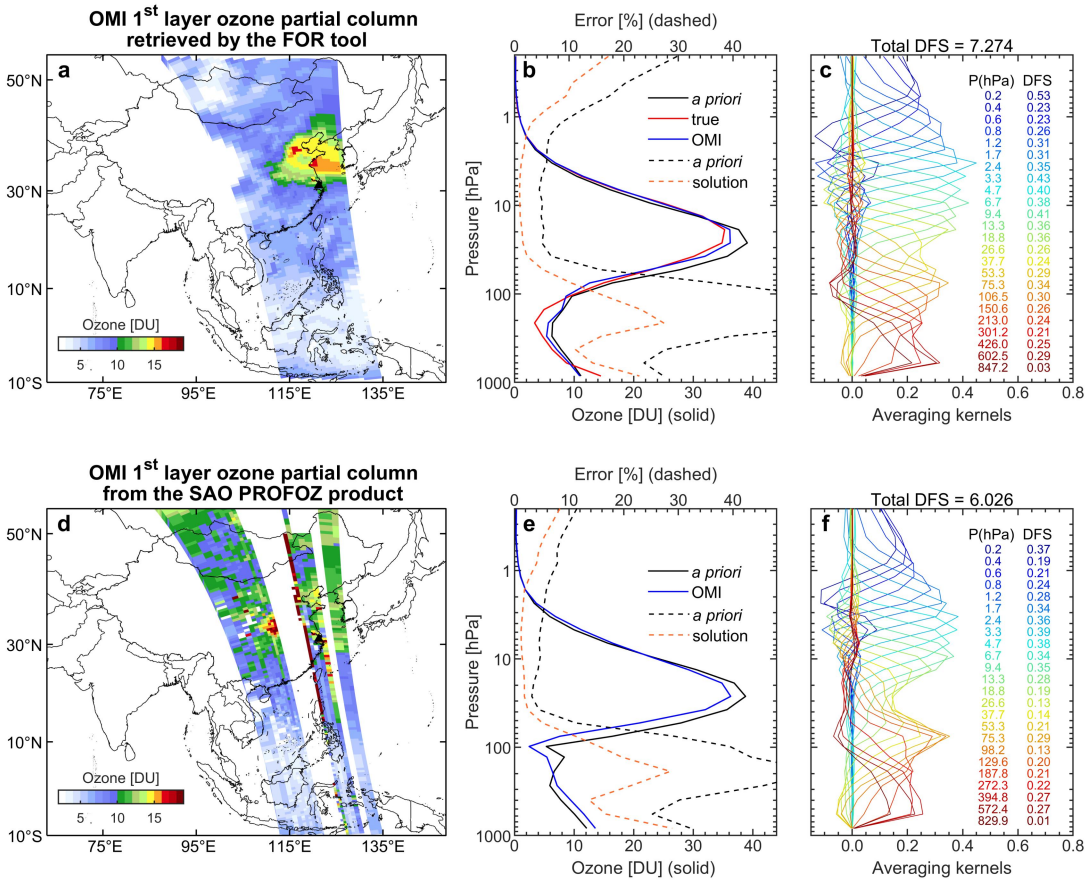

Figure S2. Comparison of surface-layer ozone partial column (left panels), vertical ozone profiles and relative retrieval errors (middle panels), and averaging kernels (right panels) at the Shanghai pixel (31.1°N 121.3°E, denoted using the black triangle in left panels) at 04:55 UTC on 16 June 2020 between the OMI retrievals simulated by the fast ozone profile retrieval simulation (FOR) tool (a–c) and from the Smithsonian Astrophysical Observatory (SAO) OMI Ozone Profile (PROFOZ) product (d–f, (https://avdc.gsfc.nasa.gov/pub/data/satellite/Aura/OMI/V03/L2/OMPROFOZ/, last access: 1 March 2023). In panels (b) and (e), the solid lines denote the *a priori* (black), true (red), and retrieved (blue) profiles. The dashed lines represent the *a priori* (black) and solution (orange) errors that both normalized to *a priori* profiles. In panels (c) and (f), the caption gives the total degree of freedom for the signal (DFS; defined as the trace of the averaging kernel matrix). Averaging kernels (colored by layers) are normalized to the thickness of each layer and *a priori* errors. Also inserted are elements of the DFS vector along with the central pressure of each layer.

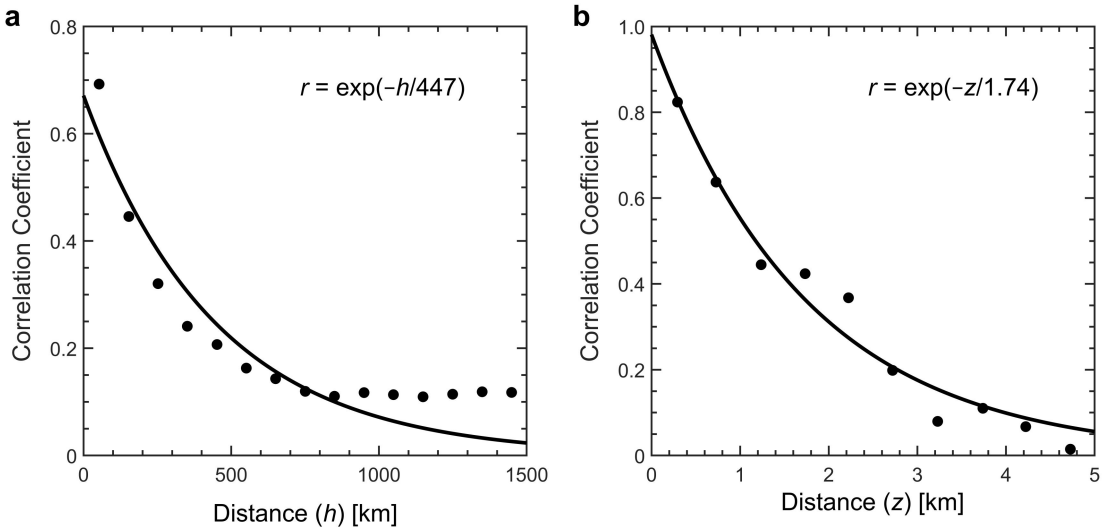

Figure S3. Horizontal and vertical error correlation length for the GEOS-Chem simulation of tropospheric ozone in Asia. Panel (a) shows the correlation coefficients (*r*) of the model errors between pairs of surface monitoring sites relative to surface ozone observations from the China National Environmental Monitoring Center (CNEMC; http://www.cnemc.cn/, last access: 1 March 2023) and plotted against the horizontal distance *h* (in km, binned every 100 km). Panel (b) shows the correlation coefficients of the model errors between pairs of vertical levels (from surface to 8 km altitude) relative to ozonesonde measurements (Shu *et al.*, 2022) and plotted against the vertical distance *z* (in km, binned every 500 m). Exponential fits based on the least-squares method to the data are shown inset.

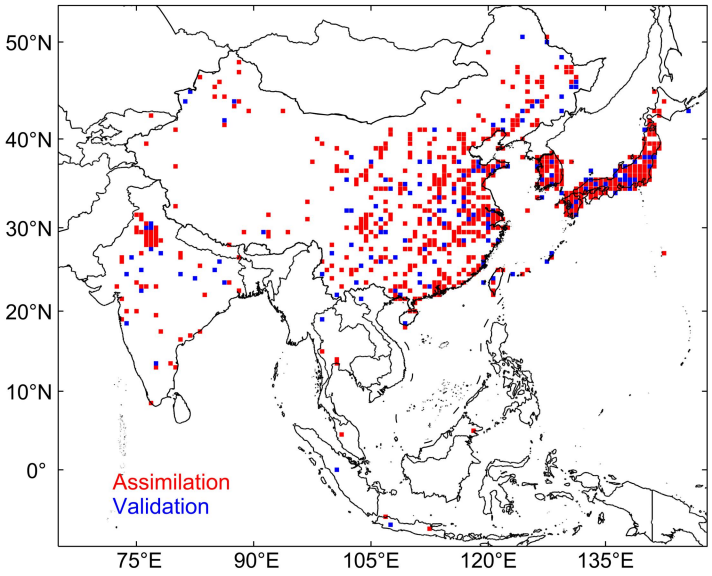

Figure S4. Distribution of super-observation grids for assimilation (red) and validation (blue) over the Asian domain.

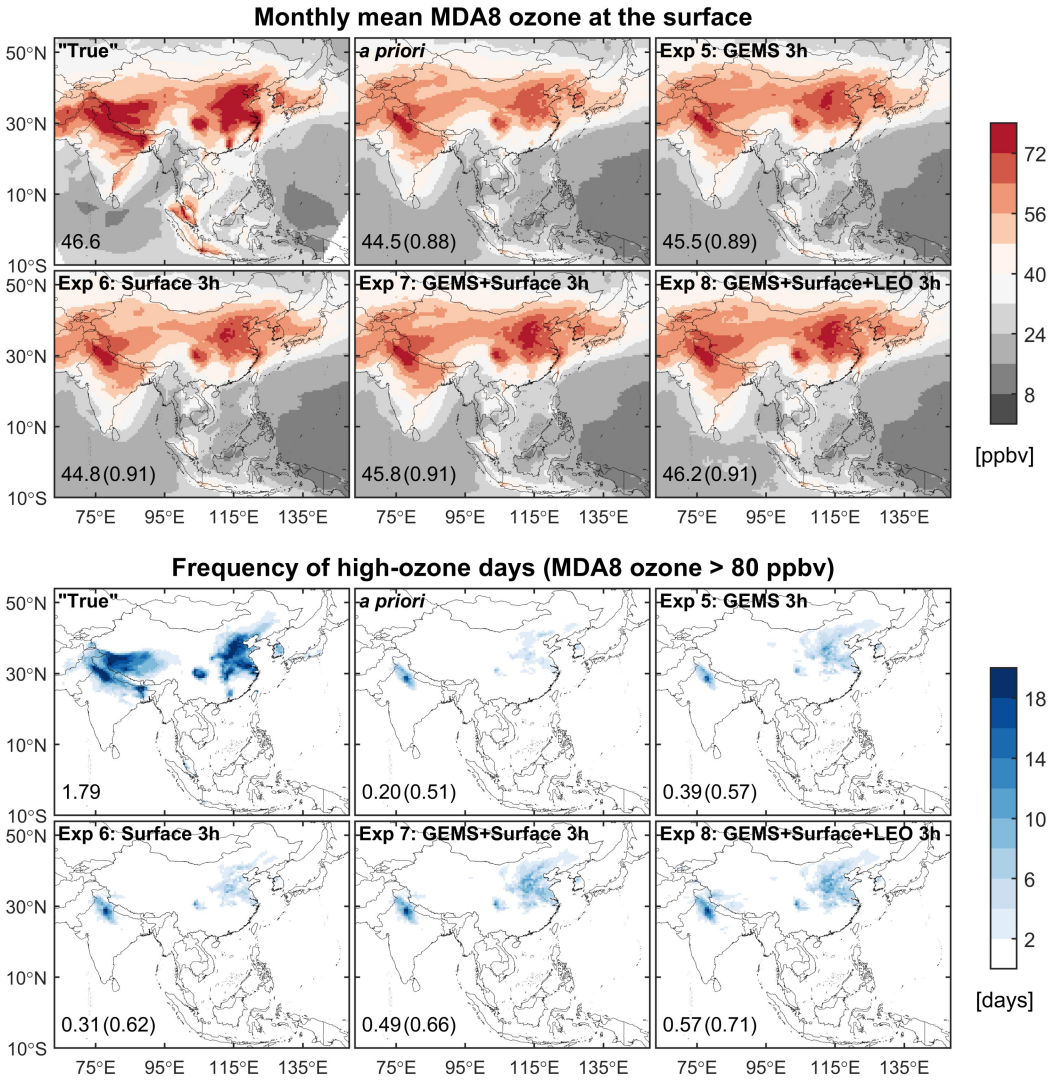

Figure S5. Same as Fig. 4 but for the *assimilation runs* with the assimilation time step of 3 h (Exp 5–8 in Table 1).

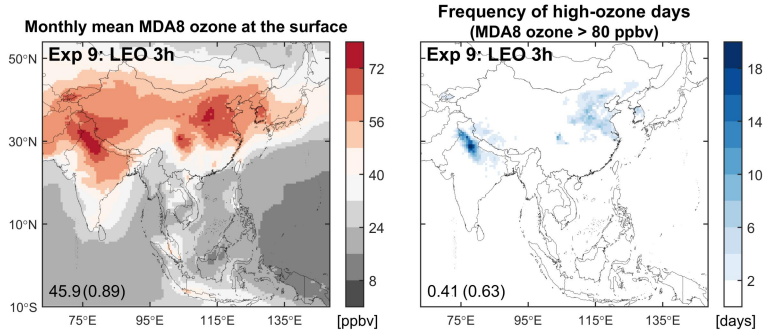

Figure S6. Same as Fig. 4 but for the *assimilation run* Exp 9 (Table 1).

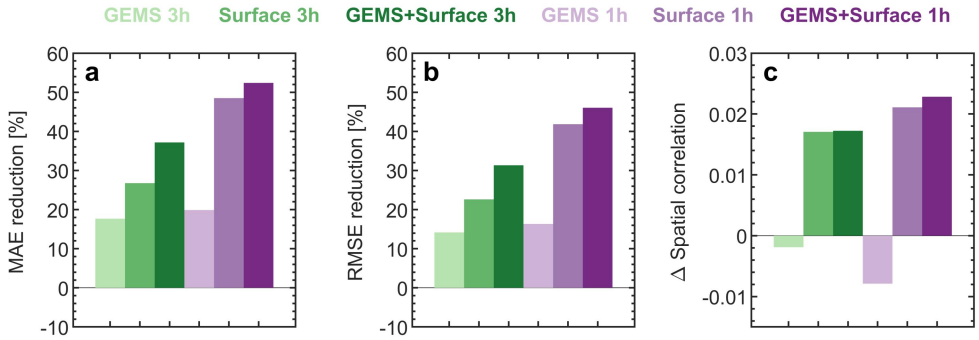

Figure S7. Same as Fig. 5 but for eastern China (20–42°N, 110–123°E).

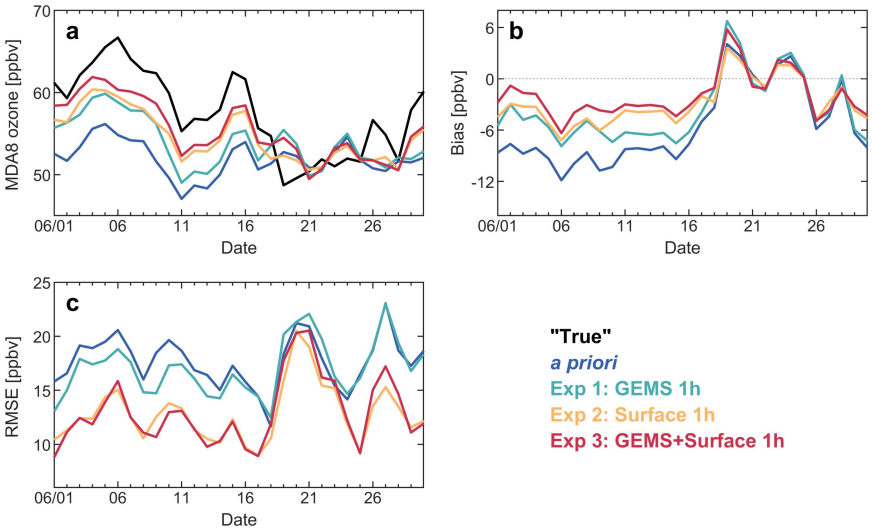

Figure S8. Same as Fig. 6a–c but for the comparison of the daily variations.

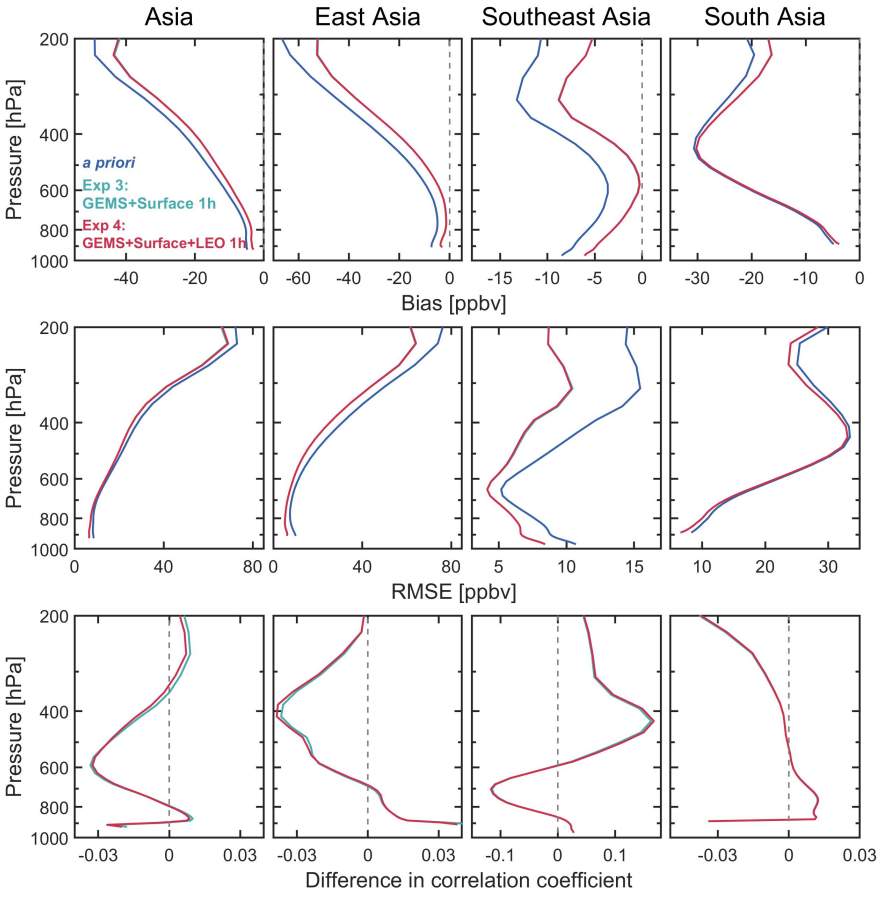

Figure S9. Same as Fig. 7 but for the *assimilation runs* with the assimilation time step of 1 h (Exp 3 and 4 in Table 1).

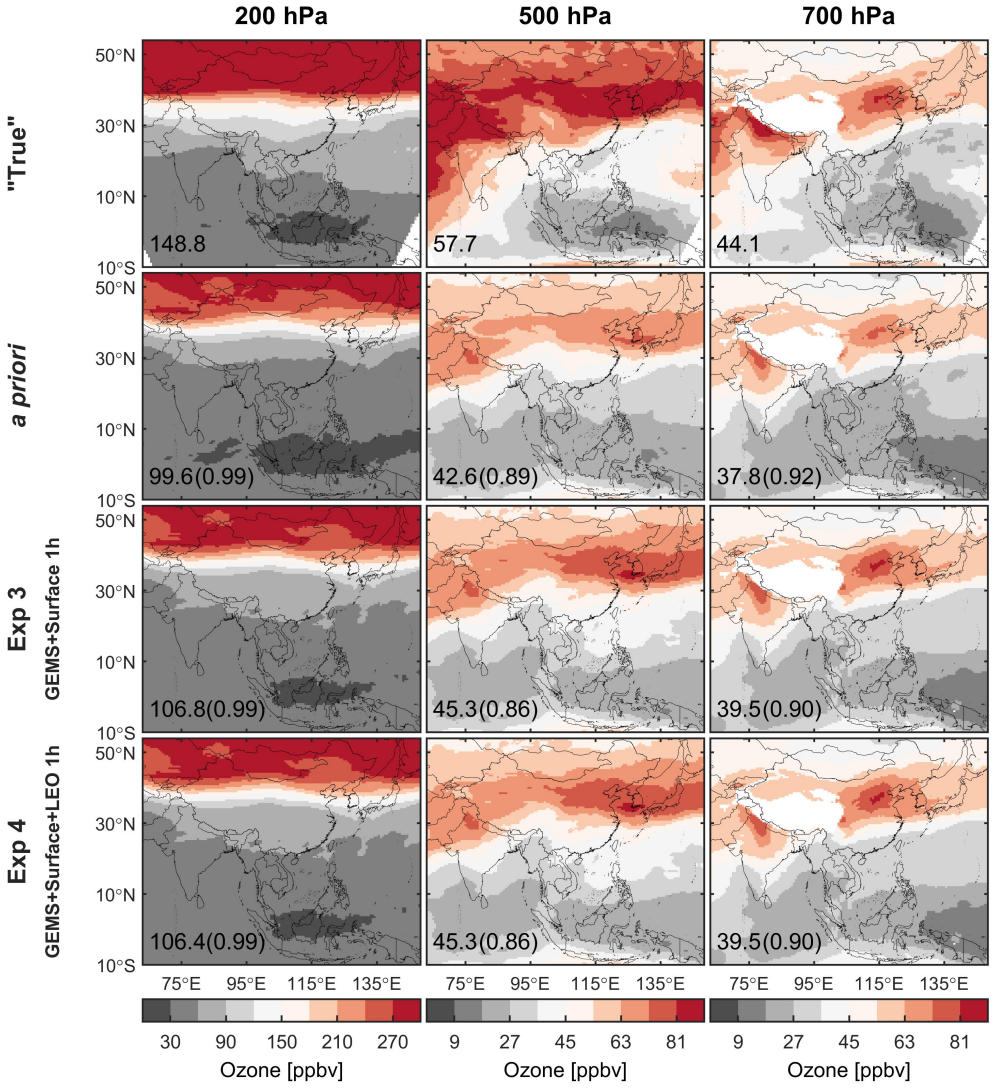

Figure S10. Same as Fig. 8 but for the *assimilation runs* with the assimilation time step of 1 h (Exp 3 and 4 in Table 1).

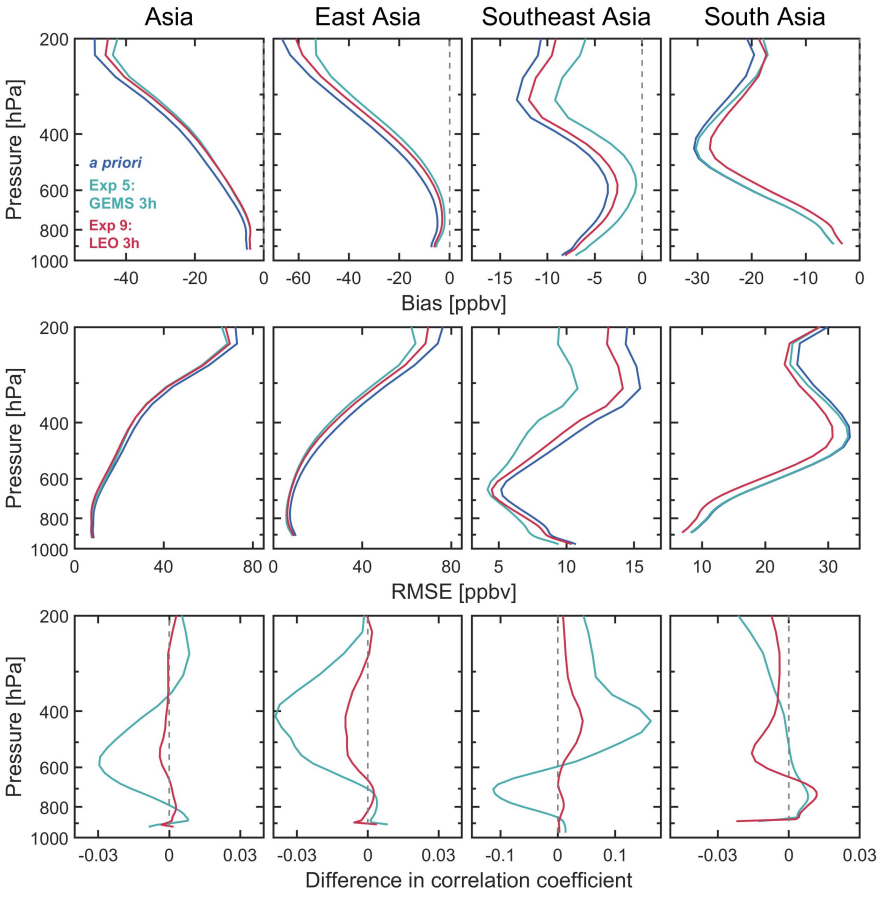

Figure S11. Same as Fig. 7 but for the *assimilation runs* Exp 5 and 9 (Table 1).

References

Bey, I., Jacob, D. J., Yantosca, R. M., Logan, J. A., Field, B. D., Fiore, A. M., Li, Q., Liu, H. Y., Mickley, L. J., and Schultz, M. G.: Global modeling of tropospheric chemistry with assimilated meteorology: Model description and evaluation, J. Geophys. Res. Atmos., 106, 23073–23095, https://doi.org/10.1029/2001JD000807, 2001.

Gelaro, R., McCarty, W., Suárez, M. J., Todling, R., Molod, A., Takacs, L., Randles, C. A., Darmenov, A., Bosilovich, M. G., Reichle, R., Wargan, K., Coy, L., Cullather, R., Draper, C., Akella, S., Buchard, V., Conaty, A., da Silva, A. M., Gu, W., Kim, G.-K., Koster, R., Lucchesi, R., Merkova, D., Nielsen, J. E., Partyka, G., Pawson, S., Putman, W., Rienecker, M., Schubert, S. D., Sienkiewicz, M., and Zhao, B.: The Modern-Era Retrospective Analysis for Research and Applications, Version 2 (MERRA-2), J. Climate, 30, 5419–5454, https://doi.org/10.1175/jcli-d-16-0758.1, 2017.

Gettelman, A., Mills, M. J., Kinnison, D. E., Garcia, R. R., Smith, A. K., Marsh, D. R., Tilmes, S., Vitt, F., Bardeen, C. G., McInerny, J., Liu, H.-L., Solomon, S. C., Polvani, L. M., Emmons, L. K., Lamarque, J.-F., Richter, J. H., Glanville, A. S., Bacmeister, J. T., Phillips, A. S., Neale, R. B., Simpson, I. R., DuVivier, A. K., Hodzic, A., and Randel, W. J.: The Whole Atmosphere Community Climate Model Version 6 (WACCM6), J. Geophys. Res. Atmos., 124, 12380–12403, https://doi.org/10.1029/2019JD030943, 2019.

Giglio, L., Randerson, J. T., and van der Werf, G. R.: Analysis of daily, monthly, and annual burned area using the fourth-generation global fire emissions database (GFED4), J. Geophys. Res. Biogeosci., 118, 317–328, https://doi.org/10.1002/jgrg.20042, 2013.

Guenther, A. B., Jiang, X., Heald, C. L., Sakulyanontvittaya, T., Duhl, T., Emmons, L. K., and Wang, X.: The Model of Emissions of Gases and Aerosols from Nature version 2.1 (MEGAN2.1): an extended and updated framework for modeling biogenic emissions, Geosci. Model Dev., 5, 1471–1492, https://doi.org/10.5194/gmd-5-1471-2012, 2012.

Hoesly, R. M., Smith, S. J., Feng, L., Klimont, Z., Janssens-Maenhout, G., Pitkanen, T., Seibert, J. J., Vu, L., Andres, R. J., Bolt, R. M., Bond, T. C., Dawidowski, L., Kholod, N., Kurokawa, J. I., Li, M., Liu, L., Lu, Z., Moura, M. C. P., O'Rourke, P. R., and Zhang, Q.: Historical (1750–2014) anthropogenic emissions of reactive gases and aerosols from the Community Emissions Data System (CEDS), Geosci. Model Dev., 11, 369–408, https://doi.org/10.5194/gmd-11-369-2018, 2018.

Janssens-Maenhout, G., Crippa, M., Guizzardi, D., Dentener, F., Muntean, M., Pouliot, G., Keating, T., Zhang, Q., Kurokawa, J., Wankmüller, R., Denier van der Gon, H., Kuenen, J. J. P., Klimont, Z., Frost, G., Darras, S., Koffi, B., and Li, M.: HTAP_v2.2: a mosaic of regional and global emission grid maps for 2008 and 2010 to study hemispheric transport of air pollution, Atmos. Chem. Phys., 15, 11411–11432, https://doi.org/10.5194/acp-15-11411-2015, 2015.

Li, M., Zhang, Q., Kurokawa, J. I., Woo, J. H., He, K., Lu, Z., Ohara, T., Song, Y., Streets, D. G., Carmichael, G. R., Cheng, Y., Hong, C., Huo, H., Jiang, X., Kang, S., Liu, F., Su, H., and Zheng, B.: MIX: a mosaic Asian anthropogenic emission inventory under the international collaboration framework of the MICS-Asia and HTAP, Atmos. Chem. Phys., 17, 935–963, https://doi.org/10.5194/acp-17-935-2017, 2017.

Mao, J., Paulot, F., Jacob, D. J., Cohen, R. C., Crounse, J. D., Wennberg, P. O., Keller, C. A., Hudman, R. C., Barkley, M. P., and Horowitz, L. W.: Ozone and organic nitrates over the eastern United States: Sensitivity to isoprene chemistry, J. Geophys. Res. Atmos., 118, 11,256–211,268, https://doi.org/10.1002/jgrd.50817, 2013.

Park, R. J., Jacob, D. J., Field, B. D., Yantosca, R. M., and Chin, M.: Natural and transboundary pollution influences on sulfate-nitrate-ammonium aerosols in the United States: Implications for policy, J. Geophys. Res. Atmos., 109, https://doi.org/10.1029/2003JD004473, 2004.

Shu, L., Zhu, L., Bak, J., Zoogman, P., Han, H., Long, X., Bai, B., Liu, S., Wang, D., Sun, W., Pu, D., Chen, Y., Li, X., Sun, S., Li, J., Zuo, X., Yang, X., and Fu, T.-M.: Improved ozone simulation in East Asia via assimilating observations from the first geostationary air-quality monitoring satellite: Insights from an Observing System Simulation Experiment, Atmos. Environ., 274, 119003, https://doi.org/10.1016/j.atmosenv.2022.119003, 2022.

Wiedinmyer, C., Akagi, S. K., Yokelson, R. J., Emmons, L. K., Al-Saadi, J. A., Orlando, J. J., and Soja, A. J.: The Fire INventory from NCAR (FINN): a high resolution global model to estimate the emissions from open burning, Geosci. Model Dev., 4, 625–641, https://doi.org/10.5194/gmd-4-625-2011, 2011.

Zaveri, R. A., and Peters, L. K.: A new lumped structure photochemical mechanism for large-scale applications, J. Geophys. Res. Atmos., 104, 30387–30415, https://doi.org/10.1029/1999JD900876, 1999.

Zaveri, R. A., Easter, R. C., Fast, J. D., and Peters, L. K.: Model for Simulating Aerosol Interactions and Chemistry (MOSAIC), J. Geophys. Res. Atmos., 113, https://doi.org/10.1029/2007JD008782, 2008.

Zheng, B., Tong, D., Li, M., Liu, F., Hong, C., Geng, G., Li, H., Li, X., Peng, L., Qi, J., Yan, L., Zhang, Y., Zhao, H., Zheng, Y., He, K., and Zhang, Q.: Trends in China's anthropogenic emissions since 2010 as the consequence of clean air actions, Atmos. Chem. Phys., 18, 14095–14111, https://doi.org/10.5194/acp-18-14095-2018, 2018.